Journal of Applied Electrochemistry (2006) 36:1169–1173
DOI 10.1007/s10800-006-9192-1

Electrodeposition of aluminum from molten $AlCl_3$–NaCl–KCl mixture

M. JAFARIAN[1,*], M. G. MAHJANI[1], F. GOBAL[2] and I. DANAEE[1]
[1]*Departement of chemistry, K.N. Toosi University of Technology, 15875-4416Tehran, Iran*
[2]*Departement of chemistry, Sharif University of Technology, 11365-9516Tehran, Iran*
*(*author for correspondence, e-mail: mjafarian@kntu.ac.ir)*

Received 8 November 2005; accepted in revised form 6 July 2006

Key words: aluminum, diffusion coefficient, electrodeposition, KI, molten salt

Abstract

Electrochemical deposition of aluminum from basic and acidic molten NaCl-KCl-$AlCl_3$ mixture on a graphite electrode at 140 °C was studied by voltammetry, chronopotentiometry and constant current deposition. The deposition of aluminum was found to proceed via a nucleation/growth mechanism in basic melt, while it was found to be diffusion controlled in acidic melt. The diffusion coefficient calculated for $Al_2Cl^-_7$ ions in acidic melt by voltammetry was in agreement with the deductions of voltammetry. The morphology of the aluminum deposits was examined using a metallographic microscope and by SEM. It was shown that, depending on the current density (c.d.) and $AlCl_3$ concentration (acidic or basic melt) different aluminum morphologies were evident but a silver-bright, compact, and very stable metallic form of aluminum deposit was obtained in acidic melt with KI addition as surfactant.

1. Introduction

Aluminum cannot be electrodeposited from aqueous solution or from any protic solvent due to the decomposition of the solvent which occurs at potentials more positive than that of Al deposition. A number of non-aqueous solvent/electrolyte systems have been examined for the low-temperature electrodeposition of aluminum [1, 2]. Aluminum can be electrodeposited from three types of non-aqueous solution: (i) mixtures of AlX_3 (X = Br or Cl) with alkali metals or various organic halide salts or with aromatic hydrocarbon solvents [3], (ii) mixtures of aluminum hydrides such as $LiAlH_4$ and $AlCl_3$ dissolved in ethers [4], and (iii) mixtures of $Al(C_2H_5)_3 + NaF$ in toluene at 80 °C [5]. Low temperature haloaluominate molten salts [6–10] fall into the first category. In this category, numerous reports describing the electrodeposition of aluminum from the Lewis acidic molten salt systems $AlCl_3$–(Bupy)Cl or –Me(Etim)Cl have appeared[11–15]. Most of these studies are concerned with the kinetics and mechanism of aluminum electrodeposition and/or stripping of aluminum off the inert electrodes such as glassy carbon, mercury, platinum, and tungsten. Fewer reports have appeared for alkali metal molten salt studies [6–10].

The following equilibrium [16] exists in an $AlCl_3$: MCl system, where M represents alkali metal ions or organic onium ions:

$$2AlCl^-_4 \Leftrightarrow Al_2Cl^-_7 + Cl^- \quad (1)$$

In basic melts, the Al- containing ion is mainly present as $AlCl^-_4$, whereas in acidic melts the $Al_2Cl^-_7$ ion becomes predominant. In inorganic melts, aluminum deposition proceeds through the discharge of either $AlCl^-_4$ or $Al_2Cl^-_7$ ions. In basic melts, the deposition reaction involves the discharge of $AlCl^-_4$ ions:

$$AlCl^-_4 + 3e^- \Leftrightarrow Al + 4Cl^- \quad (2)$$

while in acidic melts, $Al_2Cl^-_7$ is the species that is reduced to give Al deposit:

$$4Al_2Cl^-_7 + 3e^- \Leftrightarrow Al + 7AlCl^-_4 \quad (3)$$

In studies on aluminum refining at fairly low temperatures in NaCl–$AlCl_3$ melts, Midorikawa [17] found that a lead plate was the most favorable cathode material for the formation of compact, smooth and adherent aluminum deposits, followed by zinc, copper, iron, silver, aluminum, magnesium and carbon. Aluminum deposits on a carbon plate were never adherent but were powdery in the absence of surfactant. Electrode substrate [18], inorganic and organic additives [17, 19] and superposed alternating [17] or pulsed current [10] also have significant effects on the inhibition of aluminum dendrite formation.

During the charging of a rechargeable battery based on aluminum anodes, Hejuler et al. [6–8] found that aluminum dendrites and spongy deposits can be formed under certain circumstances. The spacing between the electrodes in batteries is usually very small; hence, the

density of the deposits is of importance for the capacity and life of the batteries. Non-compact, dendritic deposits may cause short circuiting, early deterioration and so on. It was also found that the spongy deposits can be inhibited by using pulsed current deposition or by adding manganese chloride to the melt. Al–Mn alloy was formed under the latter condition

Little work has been reported in the NaCl–KCl–$AlCl_3$ melt [9, 10]. Hayshi et al. [10] found that the main component of cathodic polarization in a NaCl–KCl–$AlCl_3$ melt was crystallization overvoltage in the low polarization potential region

It was our intention to study the electrochemical deposition of aluminum from acidic and basic NaCl–KCl–$AlCl_3$ molten salt. This system can be of great significance from the technical point of view because of its low vapor pressure and its low melting point of 115 °C.

2. Experimental

Materials used in this work were analytical grade of Merck origin. $AlCl_3$ was distilled while NaCl and KCl were dried at 300 °C prior to use. Fused electrolyte with the composition 66–20–14 wt% ($AlCl_3$–NaCl–KCl) had a melting point of 115 °C [9, 10]. The studies were performed at 140 °C. The experiments were carried out in a conventional three electrode cell with a hand polished graphite rod exposing 0.5 cm^2 area forming the working electrode. Its potential was monitored against an aluminum (99.999% purity) reference electrode directly immersed in the melt [20]. A large graphite rod was used as the counter electrode. The electrochemical cell was powered by an EG&G model 273A potentiostat/galvanostat run by a PC through M270 commercial software and cyclic voltammetry (CV) and chronopotentiometry (CP) were carried out. Details of the experimental set up are given elsewhere [20, 21]

3. Result and discussion

3.1. *Basic electrochemical studies*

Figure 1 presents a cyclic voltammogram obtained in the potential range 0.6 to -1.2 V/Al at 140 °C (without IR drop correction) with scan rate 60 mV s^{-1}. The electroactive entity, probably $AlCl_4^-$, starts to reduce at -0.81 V/Al. In the reverse scan the cross-over loop signifying nucleation/growth in the course of a cathodic scan [22] is accompanied by the anodic dissolution peak of Al at -0.27 V/Al.

The current step method is also a useful means of detecting the presence of nucleation. Potential maxima at the beginning of the transition time can be attributed to the nucleation process [23]. The experimental chronopotentiograms exhibit a characteristic maximum in the early stages of deposition as shown in Figure 2. At

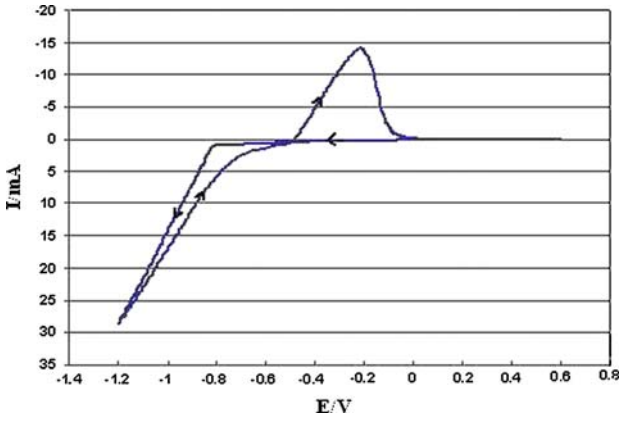

Fig. 1. Cyclic voltammogram of the graphite electrode in basic molten salt (140 °C).The scan began at 0.6 V/Al with a scan rate of 60 mV s^{-1}. Electrode area 0.5 cm^2.

the very beginning of the chronopotentiogram, the steep falling potential has contributions of both double layer charging [24] as well as pseudo capacitors of adsorption followed by monolayer deposition of the electroactive constituents. As the potential increases nucleation takes place [25], and an overvoltage is required to meet the galvanostatic conditions. As soon as nuclei are growing, the overvoltage for reduction decreases. The product $i_o\tau^{1/2}$ was found to decrease with increasing applied current density, i_o, showing that the deposition of aluminum in basic melts is not controlled by diffusion and the reaction appears to be confined to the surface or near surface domains [26]. The decreasing trend suggests that a preceding chemical reaction mechanism similar to that observed in the $AlCl_3$–(Bupy)Cl electrolyte prevails [16]

A typical cyclic voltammogram at a graphite electrode in a slightly acidic melt (after IR drop correction) is shown in Figure 3. The scan rate was 50 mV s^{-1} in the potential range 0.4 to -0.7 V/Al and at 140 °C. The voltammetric peak may be attributed to $Al_2Cl_7^-$ reduction. The peak current increases with scan rate and with $Al_2Cl_7^-$ concentration. This peak is followed by the

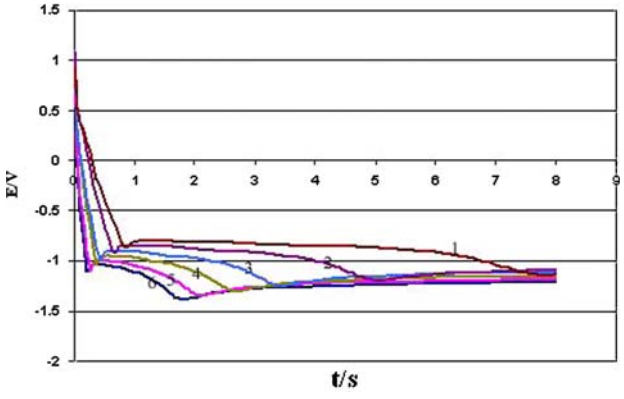

Fig. 2. Chronopotentiogram of the graphite electrode in basic melt in different current density $i_1 = 12.19$, $i_2 = 13.41$, $i_3 = 14.63$, $i_4 = 15.85$, $i = 17.07$, $i_6 = 18.29$ mA cm^{-2}.

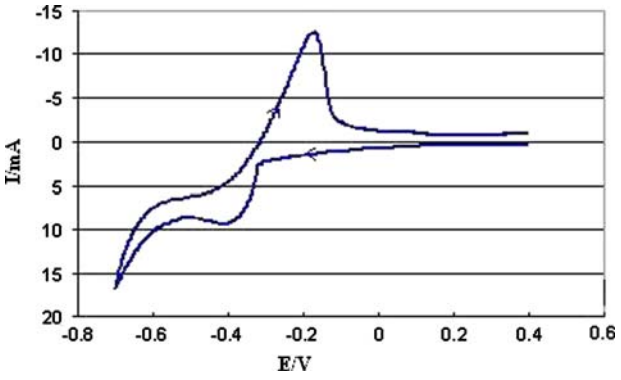

Fig. 3. Cyclic voltammogram of the graphite electrode in acidic melt (140 °C). The scan began at 0.4 V/Al with a scan rate of 50 mV s^{-1}.

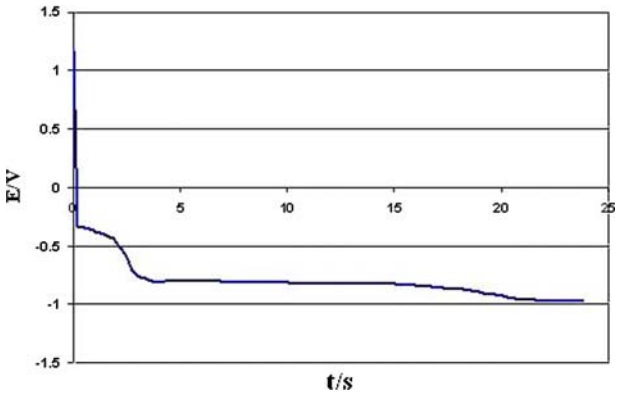

Fig. 4. Chronopotentiogram of the graphite electrode in slightly acidic melt in current density $i = 9.75$ mA cm^{-2}.

reduction of $AlCl_4^-$. Since $AlCl_4^-$ is the main anionic constituent of the solvent, its concentration does not change significantly in the acidic and basic melts. The reduction potential of $AlCl_4^-$ remains constant in the melt composition range used. When the acidity decreases the peak current decreases and shifts toward the reduction potential of $AlCl_4^-$, as expected for the case of an insoluble deposit [27]. This peak does not appear in basic melt studies indicating that only $AlCl_4^-$ is present. No overcrossing was observed in the direct and reverse scans and the dissolution peak of deposited aluminum is observed at -0.4 V/Al. Although the ratio of the anodic peak current to the cathodic peak current obtained from this figure is higher than one, the coulombic charge associated with the deposition process is nearly equal to that of the stripping process. This indicates that the deposited aluminum is an insoluble product with constant activity during the deposition and stripping process. A plot of peak current (i_p) versus the square root of scan rate (v) for the deposition process exhibits a straight line which passes through the origin within experimental error. Also, the peak potential remains constant and both features point to the diffusion-controlled nature of aluminum deposition in acidic melts. From the slope of the straight line (i_pvsv$^{1/2}$) the diffusion coefficient of $Al_2Cl_7^-$ was obtained as $D_{Al_2Cl_7^-} = 5.7 \times 10^{-6}\,cm^2\,s^{-1}$ where the concentration of $Al_2Cl_7^-$ was 8.5×10^{-5} mol cm^{-3}

Chronopotentiometric measurements were also conducted with the graphite electrode in slightly acidic melt and the results are shown in Figure 4 where two steps appear in the Chronopotentiograms (after IR drop correction). The first step is related to $Al_2Cl_7^-$ reduction and is at a potential in agreement with that of the corresponding process in the cyclic voltammogram. The second step is related to $AlCl_4^-$ reduction in acidic melt. At the transition time $\tau = 2.09$ s, the potential rises sharply as the concentration of electroactive species at the electrode surface reaches zero. The first step of $Al_2Cl_7^-$ reduction at different currents are shown in Figure 5. The product $i_o\tau^{1/2}$ was found to be constant with increasing current density, i_o, showing that $Al_2Cl_7^-$ reduction is controlled by diffusion and Sand's law is obeyed. The diffusion coefficient deduced from Sand's law is in very good agreement with the deduction from voltammetry and is found to be $D_{Al_2Cl_7^-} = 5 \times 10^{-6}\,cm^2\,s^{-1}$. Logarithmic analyses of chronopotentiograms obtained in diffusion controlled region gave good linear fits for the insoluble product model where the plot of E vs $\ln(\tau^{1/2} - t^{1/2})/\tau^{1/2}$ is linear and from the slopes of this, the average value of n was calculated to be 0.75 ± 0.01 in agreement with expectations from the equilibrium (3) (eq. (4))

$$E = E_{th} + \frac{RT}{nF}\ln\left(\frac{\tau^{1/2} - t^{1/2}}{\tau^{1/2}}\right) \tag{4}$$

3.2. *Constant current deposition studies*

Aluminum deposits obtained by electrochemical reduction from basic melt can vary greatly in their appearance depending on the deposition conditions. Without additive in the basic melt the aluminum was dull grey, spongy and unstable, as can be seen from the micrograph of Figure 6. It was found that in the range 130–200 °C, temperature had little effect on the quality of the

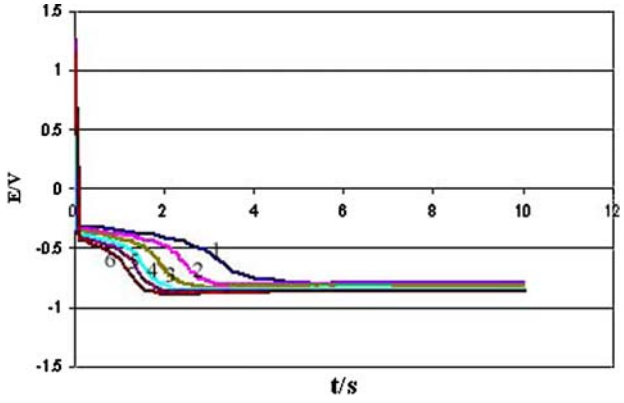

Fig. 5. Chronopotentiogram of the graphite electrode in slightly acidic melt in different current density $i_1 = 8.53$, $i_2 = 9.75$, $i_3 = 10.97$, $i_4 = 12.19$, $i_5 = 13.41$, $i_6 = 14.63$ mA cm^{-2}.

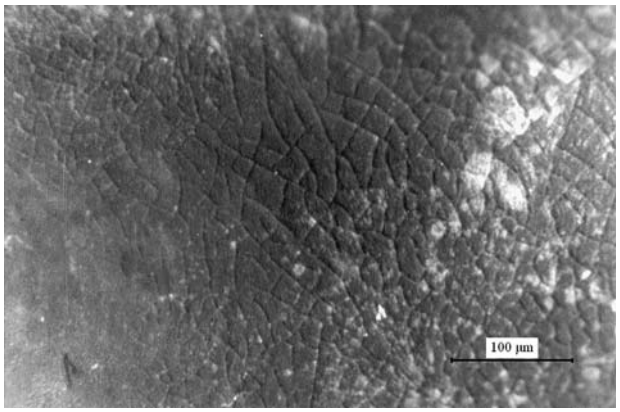

Fig. 6. Surface of aluminum deposited in basic melt in intermediate current density by metallographic microscope. Current density 0.05 A cm^{-2}, deposition time 8 h, temperature 140 °C, melt composition 66–20–14 wt%.

Al deposit while the current densities had a pronounced effect. In basic melts at 140 °C, it seems that spongy deposits are always formed at low current densities below 0.03 A cm^{-2}. At current densities between 0.03 and 0.06 A cm^{-2}, deposits appear smooth and granular but dull, dark and weakly adherent to the substrate, while at very high current densities (> 0.08 A cm^{-2}) dendrites or very porous deposits are often obtained. Aluminum grains formed during deposition can easily be observed with a microscope by using grazing illumination. It is found that the grain size of the aluminum deposits decreases as the current density increases. At a very low current density (< 0.02 A cm^{-2}), segregated aluminum particles can be obtained and spongy aluminum deposits form after prolonged deposition.

It is known from electrocrystallization theory that grain size is determined primarily by the number of nuclei formed during deposition [22]. The formation of spongy deposits at low current density can thus be attributed to the lack of nuclei initially formed to serve as growth centers. As already mentioned (Figure 1) aluminum deposition from basic molten salts proceeds via a nucleation/growth mechanism. The difficulty in electronucleation of aluminum deposits is thus assumed to be the cause of the formation of spongy deposits at low current density [17]. With increase in current density, electronucleation becomes faster and more nuclei are formed. The formation of spongy deposits is thus suppressed during subsequent growth. Smooth aluminum deposits are formed when deposition is carried out at intermediate current densities. The concentration gradient of species containing aluminum resulting from electrolysis may drive the growth of aluminum dendrites [28]. In acidic melt the deposited aluminum was smoother than that from basic melts and higher critical current densities can be used in deposition. However, a dark and non-coherent Al layer was observed. After addition of 1 wt% KI to basic melts, it was found that the quality of the aluminum film improved with increasing concentration of the salt up to 5 wt%, while further increase did not affect the quality of the Al layer. As can be seen from the metallographic micrographs (Figure 7), the deposited aluminum was macroscopically silver bright, uniform and dense. However, SEM microscopic evaluation revealed that it consisted of individual grains that are not well connected together and had little or no mechanical stability, (Figure 8). In acidic melts with addition of KI the Al layer was silver bright, compact, non-porous and very stable, even when obtained at higher current densities. The SEM micrograph of deposited aluminum is shown in Figure 9. KI is a surfactant [29] and when present its adsorption on the electrode surface promotes nucleation. Surfactants seem to block active sites on the cathode surface and result in an energetic homogenization of the surface and consequently lead to an increased number of growing nuclei. Therefore, the formation of spongy deposits is avoided.

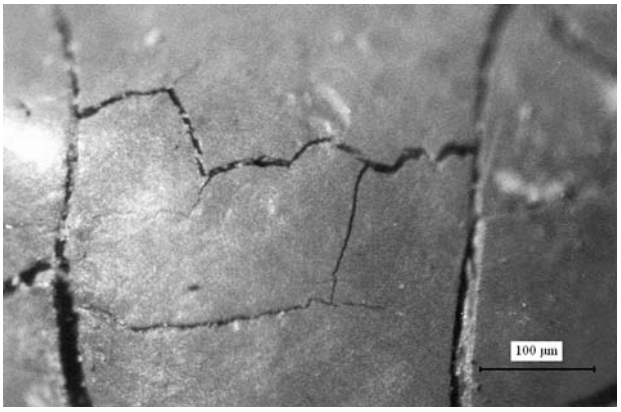

Fig. 7. Surface of aluminum deposited in basic melt with addition of 5%wt KI in intermediate current density by metallographic microscope. Current density 0.05 A cm^{-2}, deposition time 8 h, temperature 140 °C, melt composition 66–20–14 wt%.

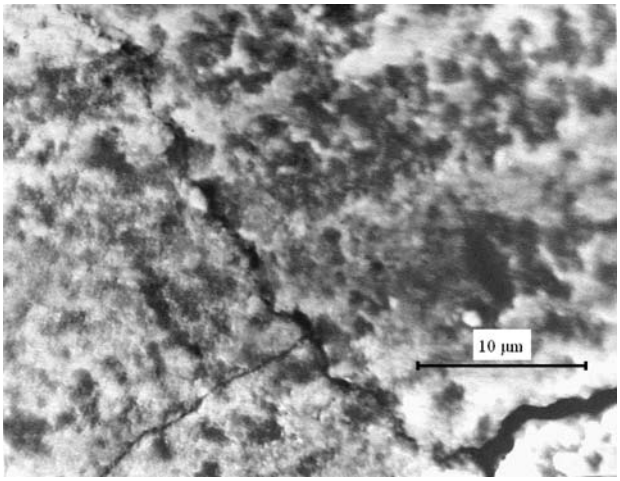

Fig. 8. Surface of aluminum deposited in basic melt with addition of 5%wt KI in intermediate current density by SEM micrograph. Current density 0.05 A cm^{-2}, deposition time 8 h, temperature 140 °C, melt composition 66–20–14 wt%.

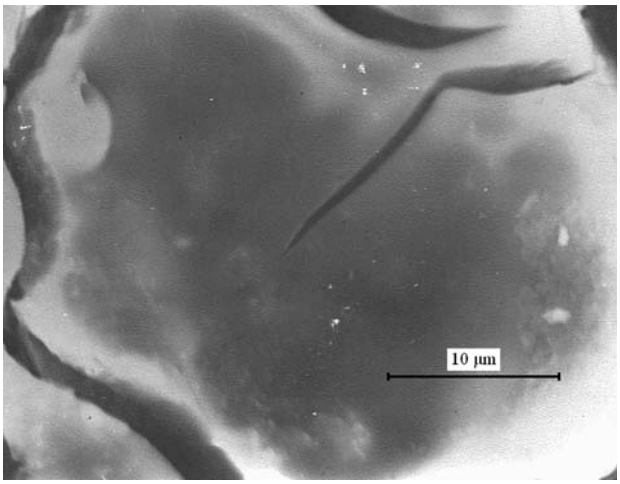

Fig. 9. Surface of aluminum deposited in acidic melt with addition of 5%wt KI in intermediate current density by SEM micrograph. Current density 0.05 A cm^{-2}, deposition time 8 h, temperature 140 °C, melt composition 66–20–14 wt%.

4. Conclusions

Electrochemical deposition of aluminum on to a graphite electrode in basic melt was found to proceed via a nucleation/growth mechanism, and deposition from acidic melts showed that $Al_2Cl^-_7$ reduction was controlled by diffusion. The diffusion coefficient of $Al_2Cl^-_7$ was obtained by voltammetry and is in agreement with the chronopotentiometry measurements and was found to be $D_{Al_2Cl_7^-} = 5.5 \times 10^{-6}\,cm^2\,s^{-1}$. Several types of aluminum deposit can be electrodeposited from the melt mainly depending on the current densities applied and the $AlCl_3$ concentration. In basic solutions the deposit morphology is dull grey, spongy and non-compact while in acidic melt smoother aluminum is formed but is still dark and non-compact. The acidic system with KI addition as surfactant is the only system where the aluminum deposit occurred as a silver bright, compact, non-porous and very stable metallic form

References

1. A. Brenner. *in* C.W. Tobias (ed.), Advances in Electrochemistry and Electrochemical Engineering 5, (John Wiley & Sons, New York, 1967), pp. 205–248.
2. H. Lehmkuhl, K. Mehler and U. Landau, *in* H. Gerischer and C.W. Tobias (eds), Advances in Electrochemical Science and Engineering 3, (VCH Publishers, New York, 1994), pp. 163–226.
3. D.B. Keyes, T.E. Phipps, W. Klabunde (1933) U.S. Patent 1,911122.
4. D.E. Couch and A.J. Brenner, *Electrochem. Soc.* **103** (1956) 657.
5. A.E. Finholt, A.C. Bond and H.I. Schlesinger, *J. Am. Chem. Soc.* **69** (1974) 1199.
6. Li Qingfeng, H.A. Hejuler, R.W. Berg and N.J. Bjerrum, *J. Electrochem. Soc.* **138** (1991) 763.
7. P. Rolland and G.J. Mamantov, *Electrochem. Soc.* **123** (1976) 1299.
8. Li Qingfeng, H.A. Hejuler, R.W. Berg and N.J. Bjerrum, *J. Electrochem. Soc.* **136** (1989) 2940.
9. R.G. Verdieck and L.F. Yntema, *J. Phys. Chem.* **46** (1942) 344.
10. P. Fellner, M. Chrenkova-Paucirova and K. Matiasovsky, *Surf Technol* **14** (1981) 101.
11. J. Robinson and R.A. Osteryoug, *J. Electrochem. Soc.* **127** (1980) 122.
12. J.J. Auborn and Y.L. Barberio, *J. Electrochem. Soc.* **132** (1985) 598.
13. Y. Chryssoulakis, J.C. Poignet and G. Manoli, *J. Appl. Electrochem.* **17** (1987) 857.
14. P.K. Lai and M. Skyllass-kazacos, *Electrochim. Acta* **32** (1987) 1443.
15. P.K. Lai and M. Skyllass-kazacos, *J. Electroanal. Chem.* **248** (1988) 431.
16. Qi-Xian Qin and M. Skyllas-Kazacos, *J. Electroanal. Chem.* **168** (1984) 193.
17. Li Qingfeng, H.A. Hjuler, R.W. Berg and N.J. Bjerrum, *J. Electrochem. Soc.* **137** (1990) 593.
18. B. Nayak and M.M. Misra, *J. Appl. Electrochem.* **7** (1977) 45.
19. Y.K. Delimarsky and N.K. Tumanova, *Electrochim. Acta* **24** (1979) 19.
20. M. Jafarian, M.G. Mahjani, F. Gobal and I. Danaee, *J. Electroanal. Chem.* **588** (2006) 190.
21. R.W. Berg, H.A. Hjuler and N.J. Bjerrum, *Inorg. Chem.* **23** (1984) 557.
22. R. Greef, R. Peat, L.M. Peter, D. Pletcher, J. Robinson, Instrumental Methods in Electrochemistry (Ellis Horwood, Chichester, 1985), ch. 9.
23. G.J. Hills, D.J. Schiffrin and J. Thompson, *J. Electrochim. Acta* **19** (1974) 657.
24. F. Lantelme and J. Chevalet, *Electroanal. Chem.* **121** (1981) 311.
25. G. Gunawardena, G. Hills, I. Montenegro and B. Scharifker, *J. Electroanal. Chem.* **138** (1982) 225.
26. G.R. Stafford and G.M. Haarberg, *Plasma & Ions* **1** (1999) 35.
27. T. Berzins and P. Delahay, *J. Am. Chem. Soc.* **75** (1953) 555.
28. Li Qingfeng, H.A. Hjuler, R.W. Berg and N.J. Bjerrum, *J. Electrochem. Soc.* **137** (1990) 2794.
29. M. Paucirova and K. Matiasovsky, *Electrodep. Surf. Treat* **3** (1975) 121.